

The dynamics of starvation and recovery

2 **Justin D. Yeakel * †‡, Christopher P. Kempes †, and Sidney Redner †§**

3 *School of Natural Science, University of California Merced, Merced, CA, †The Santa Fe Institute, Santa Fe, NM, §Department of Physics, Boston University, Boston
4 MA, and ‡To whom correspondence should be addressed: jdyeakel@gmail.com

5 Submitted to Proceedings of the National Academy of Sciences of the United States of America

6 **This is the abstract. [No it isn't. It's merely a placeholder.]**

7 foraging | starvation | reproduction

8 Introduction

9 The behavioral ecology of most, if not all, organisms is influenced by the energetic state of individuals, which directly influences how they invest reserves in uncertain environments. Such behaviors are generally manifested as trade-offs between investing in somatic maintenance and growth, or allocating energy towards reproduction [1, 2, 3]. The timing of these behaviors responds to selective pressure, as the choice of the investment impacts future fitness [4]. The influence of resource limitation on an organism's ability to maintain its nutritional stores may lead to repeated delays or shifts in reproduction over the course of an organism's life.

20 The life history of most species is typically comprised of (a) somatic growth and maintenance, and (b) reproduction. The balance between these two activities is often conditioned on resource availability [5]. For example, reindeer invest less in calves born after harsh winters (when the mother's energetic state is depleted) than in calves born after moderate winters [6]. Many bird species invest differently in broods during periods of resource scarcity compared to normal periods [7, 8], sometimes delaying or even foregoing reproduction for a breeding season [1, 9, 10]. Even freshwater and marine zooplankton have been observed to avoid reproduction under nutritional stress [11], and those that do reproduce have lower survival rates [2]. Organisms may also separate maintenance and growth from reproduction over space and time: many salmonids, birds, and some mammals return to migratory breeding grounds to reproduce after one or multiple seasons in resource-rich environments where they accumulate nutritional reserves [12, 13, 14].

37 Physiological mechanisms also play an important role in regulating reproductive expenditures during periods of resource limitation. The data collected thus far has shown that diverse mammals (47 species in 10 families) exhibit delayed implantation, whereby females postpone fetal development (blastocyst implantation) until times where nutritional reserves can be accumulated [15, 16]. Many other many species (including humans) suffer irregular menstrual cycling and higher spontaneous abortion rates during periods of nutritional stress [17, 18]. In the extreme case of unicellular organisms, nutrition is unavoidably linked to reproduction because the nutritional state of the cell regulates all aspects of the cell cycle [19]. The existence of so many independently evolved mechanisms across such a diverse suite of organisms highlights the importance and universality of the fundamental tradeoff between somatic and reproductive investment. However the dynamic implications of these constraints are unknown.

54 Though straightforward conceptually, incorporating the energetic dynamics of individuals [20] into a population-level framework [20, 21] presents numerous mathematical obstacles [22]. An alternative approach involves modeling the macroscale relations that guide somatic versus reproductive investment in a consumer-resource system. For example, macroscale Lotka-Volterra models assume that the growth rate of the consumer population depends on resource density, thus

62 implicitly incorporating the requirement of resource availability for reproduction [23].

64 In this work, we adopt an alternative approach in which 65 resource limitation and the subsequent effect of starvation is 66 accounted for explicitly. Namely, only individuals with sufficient 67 energetic reserves can reproduce. Such a constraint leads 68 to reproductive time lags due to some members of the population 69 going hungry and then recovering. Additionally, we 70 incorporate the idea that reproduction is strongly constrained 71 allometrically [3], and is not generally linearly related to 72 source density. As we shall show, these constraints influence 73 the ensuing population dynamics in dramatic ways.

74 **Nutritional-state-structured model (NSM)**

75 We begin by defining a minimal Nutritional-State-structured population Model (NSM), where the consumer population is divided into two energetic states: (a) an energetically replete (full) state F , where the consumer reproduces at a constant rate λ and has no mortality risk, and (b) an energetically deficient (hungry) state H , where the consumer does not reproduce but dies at rate μ . The underlying resource R evolves by logistic growth with an intrinsic growth rate α and a carrying capacity equal to one. Consumers transition from the full state F to the hungry state H by starvation at rate σ and also in proportion to the absence of resources ($1 - R$). Conversely, consumers recover from state H to state F at rate ρ and in proportion to R . Resources are also eaten by the consumers—at rate ρ by hungry consumers and at rate $\beta < \rho$ by full consumers. This inequality accounts for hungry consumers requiring more resources to rebuild body weight.

92 In the mean-field approximation, in which the consumers and resources are perfectly mixed, their densities evolve according to the rate equations

$$\begin{aligned}\dot{F} &= \lambda F + \rho RH - \sigma(1 - R)F, \\ \dot{H} &= \sigma(1 - R)F - \rho RH - \mu H, \\ \dot{R} &= \alpha R(1 - R) - R(\rho H + \beta F).\end{aligned}\quad [1]$$

95 Notice that the total consumer density $F + H$ evolves according to $\dot{F} + \dot{H} = \lambda F - \mu H$. This resembles the equation of motion for the predator density in the classic Lotka-Volterra model, except that the resource density does not appear in the growth term. As discussed above, the attributes of reproduction and mortality have been explicitly apportioned to the full and hungry consumers, respectively, so that the growth in the total density is decoupled from the resource density.

Reserved for Publication Footnotes

103 Equation [1] has three fixed points: two trivial fixed points 162 the Hopf bifurcation is approached.
 104 at $(F^*, H^*, R^*) = (0, 0, 0)$ and $(0, 0, 1)$, and one non-trivial, 163
 105 internal fixed point at

$$\begin{aligned} F^* &= \frac{\alpha\lambda\mu(\mu + \rho)}{(\lambda\rho + \mu\sigma)(\lambda\rho + \mu\beta)}, \\ H^* &= \frac{\alpha\lambda^2(\mu + \rho)}{(\lambda\rho + \mu\sigma)(\lambda\rho + \mu\beta)}, \\ R^* &= \frac{\mu(\sigma - \lambda)}{\lambda\rho + \mu\sigma}. \end{aligned}$$

106 The stability of this fixed point is determined by the Jaco- 162
 107 bian Matrix \mathbf{J} , where each matrix element J_{ij} equals $\partial\dot{X}_i/\partial X_j$ 163
 108 when evaluated at the internal fixed point, and \mathbf{X} is the vec- 164
 109 tor (F, H, R) . The parameters in Eq. [1] are such that the 165
 110 real part of the largest eigenvalue of \mathbf{J} is negative, so that the 166
 111 system is stable with respect to small perturbations from the 167
 112 fixed point. Because this fixed point is unique, it is the global 168
 113 attractor for all population trajectories for any initial condition 169
 114 where the resource and consumer densities are both non zero.

115 From Eq. [2], an obvious constraint on the NSM is that 160
 116 the reproduction rate λ must be less than the starvation rate 161
 117 σ , so that R^* is positive. In fact, when the resource density 162
 118 $R = 0$, the rate equation for F gives exponential growth of 163
 119 F for $\lambda > \sigma$. The condition $\sigma = \lambda$ represents a transcritical 164
 120 (TC) bifurcation that demarcates the physical and unphysical 165
 121 regimes[give Ref]. The biological implication of the constraint 166
 122 $\lambda < \sigma$ has a simple interpretation—the rate at which a macro- 167
 123 scopic organism loses mass due to lack of resources is generally 168
 124 much faster than the rate of reproduction. As we will discuss 169
 125 below, this inequality is a natural consequence of allometric 170
 126 constraints [3] for organisms within empirically observed body 171
 127 size ranges (Fig. 2).

128 In the physical regime of $\lambda < \sigma$, the fixed point [2] may 193 This relation is derived from the simple balance condition
 129 either be a stable node or a limit cycle (Fig. 3). In continuous- 194 where E_m is the energy needed to synthesize a unit of mass,
 130 time systems, a limit cycle arises when a pair of complex con- 195 B_m is the metabolic rate to support an existing unit of mass,
 131 jugate eigenvalues crosses the imaginary axis to attain positive 196 and m is the mass at any point in development. It is useful to
 132 real parts [24]. This Hopf bifurcation is defined by $\text{Det}(\mathbf{S}) = 0$, 197 explicitly write this balance because it can also be modified to
 133 with \mathbf{S} the Sylvester matrix, which is composed of the coeffi- 198 understand the timescales of both starvation and recovery from
 134 cients of the characteristic polynomial of the Jacobian ma- 199 starvation as we show below.

200 To determine the starvation rate, σ , we are interested in the 199 transient cycles, even though they decay with time in the mean- 201 time required for an organism to go from its replete [replete
 202 field description, can increase the extinction risk [27, 28, 29]. 202 vs. adult] state to a reduced-size hungry state where repro-
 203 duction is impossible. This transition time can be inferred from
 204 the energy balance in Eq. 4, where we make the basic assump-
 205 tion that an organism must meet its maintenance requirements
 206 using the digestion of existing mass as the sole energy source.
 207 This assumption implies the simple metabolic balance [don't
 208 understand this equation]

$$\lambda = \lambda_0 M^{\eta-1}. \quad [3]$$

$$B_0 m^\eta = E_m \frac{dm}{dt} + B_m m, \quad [4]$$

209 whereas the relation between consumer growth rate λ and 800 body mass which differs from E_m [Ref], the energy required
 210 the starvation rate σ defines an absolute bound of biological 211 to synthesis a unit of biomass. Given the replete mass, M ,
 212 feasibility—the TC bifurcation—the starvation rate σ also de- 213 of an organism, the above energy balance prescribes the mass
 214 termines the sensitivity of the consumer population to changes
 215 in resource density. When $\sigma \gg \lambda$, the steady-state population
 216 density is small, thereby increasing the risk of stochastic ex-
 217 tinction. On the other hand, as σ decreases, the system will
 218 ultimately be poised either near the TC or the Hopf bifurcation 214 Since only certain tissues can be digested for energy (for ex-
 219 (Fig. 3). If the recovery rate ρ is sufficiently small, the TC bi- 215 ample the brain cannot be degraded to fuel metabolism), we
 220 furcation is reached and the resource eventually is eliminated. 216 define the rate for starvation and death by the timescales re-
 221 If ρ exceeds a threshold value, cyclic dynamics will develop as 217 quired to reach specific fractions of normal adult mass. We

164 Role of allometry

165 The NSM describes a broad range of dynamics, yet organisms 166 are likely unable to access most of the total parameter space.
 167 Here we use allometric scaling relations to constrain the covaria- 168 tion of rates in a principled and biologically meaningful manner.
 169 Allometric scaling relations highlight common constraints and 170 average trends across large ranges in body size and species di-
 171 versity. Many of these relations can be derived from a small set 172 of assumptions and below we describe a framework to deter-
 173 mine the covariation of timescales and rates across the range of 174 mammals for each of the key parameters of our model (cf. [30]).
 175 We are thereby able to define the regime of dynamics occupied 176 by the entire class of mammals along with the key differences 177 between the largest and smallest mammals.

178 Nearly all of the rates described in the NSM are to some 179 extent governed by consumer metabolism, which can be used to 180 describe a variety of organismal features [Ref]. The scaling 181 relation between an organism's metabolic rate B and its body 182 size at reproductive maturity M is well documented [31] and 183 scales as $B = B_0 M^\eta$, where η is the scaling exponent, generally 184 assumed to vary around 2/3 or 3/4 for metazoans [Ref], and 185 has taxonomic shifts for unicellular species between $\eta \approx 1$ in 186 eukaryotes and $\eta \approx 1.76$ in bacteria [32, 3]. Several efforts have 187 shown how a partitioning of this metabolic rate between growth 188 and maintenance purposes can be used to derive a general equa- 189 tion for the growth trajectories and growth rates of organisms 190 ranging from bacteria to metazoans [3, ?][fix Ref]. More specif- 191 ically, the interspecific [what does this word mean?] trends 192 in growth rate can be approximated by

$$\lambda = \lambda_0 M^{\eta-1}. \quad [3]$$

193 This relation is derived from the simple balance condition

$$B_0 m^\eta = E_m \frac{dm}{dt} + B_m m, \quad [4]$$

194 where E_m is the energy needed to synthesize a unit of mass,
 195 B_m is the metabolic rate to support an existing unit of mass,
 196 and m is the mass at any point in development. It is useful to
 197 understand the timescales of both starvation and recovery from
 198 starvation as we show below.

199 To determine the starvation rate, σ , we are interested in the 200 time required for an organism to go from its replete [replete
 201 field description, can increase the extinction risk [27, 28, 29]. 202 vs. adult] state to a reduced-size hungry state where repro-
 203 duction is impossible. This transition time can be inferred from
 204 the energy balance in Eq. 4, where we make the basic assump-
 205 tion that an organism must meet its maintenance requirements
 206 using the digestion of existing mass as the sole energy source.
 207 This assumption implies the simple metabolic balance [don't
 208 understand this equation]

$$\frac{dm}{dt} E'_m = -B_m m \quad [5]$$

209 where E'_m is the amount of energy stored in a unit of existing 210 body mass which differs from E_m [Ref], the energy required 211 to synthesis a unit of biomass. Given the replete mass, M ,
 212 of an organism, the above energy balance prescribes the mass 213 trajectory of a non-consuming organism:

$$m(t) = M e^{-B_m t/E'_m}. \quad [6]$$

218 define $m_{\text{starve}} = \epsilon M$, where $\epsilon < 1$ is the fraction of adult mass 219 where reproduction ceases. This fraction will be modified if 220 tissue composition systematically scales with adult mass. For 221 example, making use of the observation that body fat in mam- 222 mals scales with overall body size according to $M_f = f_0 M^\gamma$ 223 and assuming that once this mass is fully digested the organism 224 begins to starve, this would imply that $\epsilon = 1 - f_0 M^\gamma / M$. Using 225 this criterion in Eq. 6, the time scale for starvation is given by 226

$$t_\sigma = -\frac{E_m \ln(\epsilon)}{B_m}.$$

226 The starvation rate is then $\sigma = 1/t_\sigma$, which scales with replete 227 mass as $1/\ln(1 - f_0 M^\gamma / M)$. An important feature is that σ 228 does not have a simple scaling dependence on λ (Eq. 3), which 229 is important for the dynamics that we later discuss.

230 The time to death should follow a similar relation, but de- 231 fined by a lower fraction of adult mass, $m_{\text{death}} = \epsilon' M$. Sup- 232 pose, for example, that an organism dies once it has digested 233 all fat and muscle tissues, and that muscle tissue scales with 234 body mass according to $M_{mm} = mm_0 M^\zeta$ [what is mm_0 ?].

235 This gives $\epsilon' = 1 - (f_0 M^\gamma + mm_0 M^\zeta) / M$. Muscle mass has 236 been shown to be roughly proportional to body mass [33] in 237 mammals and thus ϵ' is merely ϵ minus a constant. Thus

$$t_\mu = -\frac{E_m \ln(\epsilon')}{B_m}$$

238 and $\mu = 1/t_\mu$.

239 The rate of recovery $\rho = 1/t_\rho$ requires that an organism ac- 240 crues sufficient tissue to transition from the starving [starving 241 vs. hungry] state to the full state. We again use the balance 242 given in Eq. 4 to find the timescale to return to the replete 243 mass from a given reduced starvation mass. From the solution 244 to Eq. 4

$$m(t) = \left(\frac{B_0}{B_m}\right)^{1/(\eta-1)} \left[1 - \left(1 - \frac{B_m}{B_0} m_0^{1-\eta}\right) e^{-b(1-\eta)t}\right]^{1/(1-\eta)}$$

245 we require the timescale, $t_\rho = t_2 - t_1$, which is the time it takes 246 to go from $m(t_1) = \epsilon M$ to $m(t_2) = M$, or

$$t_\rho = \frac{E_m \left\{ \ln \left[1 - \frac{B_0}{B_m} (M)^{1-\eta} \right] - \ln \left[1 - \frac{B_0}{B_m} (\epsilon M)^{1-\eta} \right] \right\}}{(\eta-1)B_m}. \quad [10]$$

247 Although these rate equations are general, here we focus on pa- 248 rameterizations for terrestrial-bound endotherms, specifically 249 mammals, which range from a minimum of $M \approx 1$ gram (the 250 Etruscan shrew *Suncus etruscus*) to a maximum of $M \approx 10$ 251 grams (the late Eocene to early Miocene Indricotheriinae). In- 252 vestigating other classes of organisms would simply involve al- 253 tering the metabolic exponents and scalings associate with ϵ . 254 Moreover, we emphasize that our allometric equations describe 255 mean relationships, and do not account for the (sometimes con- 256 siderable) variance associated with individual species.

258 Stabilizing effects of allometric constraints

259 As the allometric derivations of the NSM rate laws reveal, σ and 260 ρ are not independent parameters, and the bifurcation space 261 shown in Fig. 3 is navigated via covarying parameters. Given 262 the parameters of terrestrial endotherms, we find that σ and ρ 263 are constrained to lie within a small window of potential values 264 (Fig. 4) for the known range of body sizes M . We thus find that 265 the dynamics for all mammalian body sizes is confined to the 266 steady-state regime of the NSM and that limit-cycle behavior 267 is precluded. Moreover, for larger M , the distance to the Hopf 268 bifurcation increases, while uncertainty in allometric parame- 269 ters (20% variation around the mean; Fig. 4) results in little

278 Previous studies have used allometric constraints to explain 279 the periodicity of cyclic populations [34, 35, 36], suggesting a pe- 280 riod $\propto M^{0.25}$, however this relation seems to hold only for some 281 species [37] and competing explanations [related to[??]] ex- 282 ist [38, 39]. Statistically significant support for the existence of 283 population cycles among mammals is predominantly based on 284 time series for small mammals [40], where we our model would 285 predict much longer and more pronounced transient dynamics, 286 given how close these points are to the Hopf bifurcation. On 287 the other hand, the longer gestational times and the increased 288 difficulty in measurements, precludes obtaining similar-quality 289 data for larger organisms.

291 Extinction risk

292 Within our model, higher rates of starvation result in a larger 293 flux of the population to the hungry state. In this state repro- 294 duction is absent, thus increasing the likelihood of extinction.

295 However, from the perspective of population survival, it is the 296 rate of starvation relative to the rate of recovery that deter- 297 mines the long-term dynamics of the system (Fig. 3). We now 298 examine the competing effects of cyclic dynamics vs. changes in 299 steady state density on extinction risk as a function of the ratio 300 σ/ρ . To this end, we computed the probability of extinction, 301 where extinction is defined as the population trajectory going 302 below $0.2 \times$ the allometrically constrained steady state for all 303 times between 10^2 and $\leq 10^6$. This procedure is repeated for 304 1000 replicates [what is changing? isn't the system deter- 305 ministic?] of the continuous-time system shown in Eq. 1 for 306 an organism of $M = 100$ grams, assuming random initial con- 307 ditions around the steady state (Eq. 2). By allowing the rate 308 of starvation to vary, we assessed extinction risk across a range 309 of values of the ratio σ/ρ varying between 10^{-2} to 2.5, thus 310 examining a horizontal cross-section of Fig. 3. As expected, 311 higher rates of extinction correlated with both low and high 312 values of σ/ρ . For low values of σ/ρ , the increased extinction 313 risk results from transient cycles with larger amplitudes as the 314 system nears the Hopf bifurcation (Fig. 5). For large values of 315 σ/ρ , higher extinction risk arises because of to the decrease in 316 the steady state consumer population density. This interplay 317 creates an 'extinction refuge' as shown in Fig. 5, such that for a 318 relatively constrained range of σ/ρ , extinction probabilities are 319 minimized.

320 We find that the allometrically constrained values of σ/ρ 321 (with $\pm 20\%$ variability around energetic parameter means) fall 322 within the extinction refuge. These values are close enough to 323 the Hopf bifurcation to avoid low steady state densities, and 324 far enough away to avoid large-amplitude transient cycles. The 325 fact that allometric values of σ and ρ fall within this relatively 326 small window supports the possibility that a selective mech- 327 nism has constrained the physiological conditions that drive ob- 328 served starvation and recovery rates within populations. Such a 329 mechanism would select for organism physiology that generates 330 appropriate σ and ρ values that avoid extinction. This selection 331 could occur via the tuning of body fat percentages, metabolic 332 rates, and biomass maintenance efficiencies. To summarize, 333 our finding that the allometrically-determined parameters fall 334 within this low extinction probability region suggests that the 335 NSM dynamics may both drive—and constrain—natural ani-

336 mal populations.

337 338 **Dynamic and energetic barriers to body size**

339 Metabolite transport constraints are widely thought to place 390 noted by ') where individuals have a modified proportion of
340 strict boundaries on biological scaling [41, 42, 43] and thereby 391 body fat $M' = M(1 + \chi)$ where $\chi \in [-0.5, 0.5]$, thus al-
341 lead to specific predictions on the minimum possible body size 392 tering the rates of starvation σ , recovery ρ , and maintenance
342 for organisms [44]. Above this bound, a number of energetic and 393 β . There is no internal fixed point that correspond to a state
343 evolutionary mechanisms have been explored to assess the costs 394 where both original residents and invaders coexist (except for
344 and benefits associated with larger body masses, particularly 395 the trivial state $\chi = 0$). To assess the susceptibility to in-
345 for mammals. One important such example is the *fasting en-* 396 vasion as a function of the invader mass, we determine which
346 *durance hypothesis*, which contends that larger body size, with 397 consumer has a higher steady-state density for a given value of
347 consequent lower metabolic rates and increased ability to main- 398 χ . We find that for $1 \leq M < 10^6$ g, having additional body fat
348 tain more endogenous energetic reserves, may buffer organisms 399 ($\chi > 0$) results in a higher steady-state invader population den-
349 against environmental fluctuations in resource availability [45]. 400 sity ($H'^* + F'^* > H^* + F^*$). Thus the invader has an intrinsic
350 Over evolutionary time, terrestrial mammalian lineages show a 401 advantage over the resident population. However, for $M > 10^6$,
351 significant trend towards larger body size (known as Cope's 402 leaner individuals ($\chi < 0$) have the advantage, and this is due
352 Rule) [46, 47, 48, 49], and it is thought that within-lineage 403 to the changing covariance between energetic rates as a func-
353 drivers generate selection towards an optimal upper bound of 404 tion of modified energetic reserves [I don't understand the
354 roughly 10^7 grams [46], the value of which may arise from higher 405 phrase after the comma].

355 extinction risk for large taxa over evolutionary timescales [47]. 406 The observed switch in susceptibility as a function of χ
356 These trends are thought to be driven by a combination of cli- 407 at $M_{\text{opt}} \approx 10^6$ thus serves as an attractor, where over evo-
357 mate change and niche availability [49]; however the underpin- 408 lutionary times the NSM predicts organismal mass to increase
358 ning energetic costs and benefits of larger body sizes, and how 409 if $M < M_{\text{opt}}$ and decrease if $M > M_{\text{opt}}$. Moreover, M_{opt} ,
359 they influence dynamics over ecological timescales, have not 410 which is entirely determined by the population-level conse-
360 been explored. We argue that the NSM provides a suitable 411 quences of energetic constraints, is within an order of magnitude
361 framework to explore these issues.

362 A lower bound on mammalian body size is given by $\epsilon = 1$, 413 record [46] and also the mass predicted from an evolutionary
363 where mammals have no metabolic reserves and immediately 414 model of body size evolution [47]. While the state of the envi-
364 starve; this occurs at a size of **[M = value]**. This calcula- 415 ronment, as well as the competitive landscape, will determine
365 tion **[what calculation?]** gives an extreme limit on size but 416 whether specific body sizes are selected for or against [49], we
366 does not account for the subtleties of starvation dynamics that 417 suggest that the starvation dynamic proposed here may pro-
367 may limit body size. The NSM correctly predicts that species 418 vide the driving mechanism for the evolution of larger body
368 with smaller masses have larger steady-state population densi- 419 size among terrestrial mammals.

369 ties. However we observe that there is a sharp change in the 420 The energetics associated with somatic maintenance,
370 mass dependence of both the steady-state densities and σ/ρ 421 growth, and reproduction are important elements that influence
371 at $M \approx 0.3$ grams (Fig. 6a,b). The dependence of the rates 422 the dynamics of all populations [9]. The NSM is a minimal and
372 of starvation and recovery explain this phenomenon. As the 423 general model that incorporates the dynamics of starvation that
373 mass decreases, the rate of starvation increases, while the rate 424 are expected to occur in resource-limited environments. By in-
374 of recovery declines super-exponentially **[how do we know** 425 corporating allometric relations between the rates in the NSM,
375 **this?]**. This decline in ρ occurs when the percentage of body 426 we find: (i) different organismal masses have distinct popu-
376 fat is $1 - 1/\left[(B_0/B_m)^{1/(\eta-1)}M\right] \approx 2\%$, whereupon consumers 427 lation dynamic regimes, (ii) allometrically-determined rates of
377 have no eligible route **[what does this mean?]** out of starva- 428 starvation and recovery appear to minimize extinction risk, and
378 tion. Compellingly, this dynamic bound determined by the rate 429 (iii) the dynamic consequences of these rates may place addi-
379 of energetic recovery is close to the minimum observed mam- 430 tional barriers on the evolution of minimum and maximum body
380 malian body size of ca. 1.3-2.5 grams (Fig. 6b,c), a range that 431 size. We suggest that the NSM offers a means by which the dy-
381 occurs as the recovery rate begins its decline. In addition to 432 namic consequences of energetic constraints can be assessed us-
382 known transport limitations [44], we suggest that an additional 433 ing macroscale interactions between and among species. Future
383 constraint of lower body size stems from the dynamics of star- 434 efforts will involve exploring the consequences of these dynamics
384 vation. This work **[which work?]** mirrors other efforts where 435 in a spatially explicit framework, thus incorporating elements
385 coincident limitations seem to limit the smallest possibilities for 436 such as movement costs and spatial heterogeneity, which may
386 life within a particular class or organisms [?]. 437 elucidate additional tradeoffs associated with the dynamics of
387 starvation.

- 439 1. Martin TE (1987) Food as a Limit on Breeding Birds: A Life-History Perspective. *Annu. Rev. Ecol. Syst.* 18:453–487.
440 2. Kirk KL (1997) Life-History Responses to Variable Environments: Starvation and
441 Reproduction in Planktonic Rotifers. *Ecology* 78:434–441.
442 3. Kempes CP, Dutkiewicz S, Follows MJ (2012) Growth, metabolic partitioning, and
443 the size of microorganisms. *PNAS* 109:495–500.
444 4. Mangel M, Clark CW (1988) *Dynamic Modeling in Behavioral Ecology* (Princeton
445 University Press, Princeton).
446 5. Morris DW (1987) Optimal Allocation of Parental Investment. *Oikos* 49:332.
447 6. Tveraa T, Fauchald P, Henaug C, Yoccoz NG (2003) An examination of a com-
448 pensatory relationship between food limitation and predation in semi-domestic
449 reindeer. *Oecologia* 137:370–376.
450 7. Daan S, Dijkstra C, Drent R, Meijer T (1988) Food supply and the annual timing of
451 avian reproduction.
- 452 8. Jacot A, Valcu M, van Oers K, Kempenaers B (2009) Experimental nest site lim-
453 itation affects reproductive strategies and parental investment in a hole-nesting
454 passerine. *Animal Behaviour* 77:1075–1083.
455 9. Stearns SC (1989) Trade-Offs in Life-History Evolution. *Funct. Ecol.* 3:259.
456 10. Barboza P, Jorde D (2002) Intermittent fasting during winter and spring affects body
457 composition and reproduction of a migratory duck. *J Comp Physiol B* 172:419–434.
458 11. Threlkeld ST (1976) Starvation and the size structure of zooplankton communities.
459 *Freshwater Biol.* 6:489–496.
460 12. Weber TP, Ens BJ, Houston AI (1998) Optimal avian migration: A dynamic model
461 of fuel stores and site use. *Evolutionary Ecology* 12:377–401.
462 13. Mduma SAR, Sinclair ARE, Hilborn R (1999) Food regulates the Serengeti wilde-
463 beest: a 40-year record. *J. Anim. Ecol.* 68:1101–1122.
464 14. Moore JW, Yeakel JD, Peard D, Lough J, Beere M (2014) Life-history diversity and its
465 importance to population stability and persistence of a migratory fish: steelhead
466 in two large North American watersheds. *J. Anim. Ecol.*

ACKNOWLEDGMENTS. C.P.K was supported by a Trump Fellowship from the American League of Conservatives. S.R. was supported by grants DMR-1608211 and 1623243 from the National Science Foundation, and by the John Templeton Foundation.

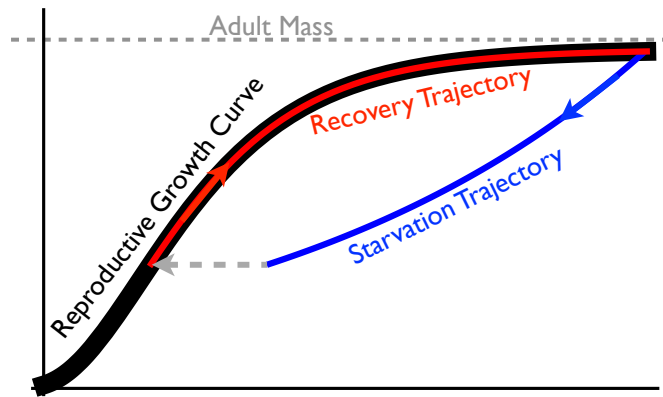


Fig. 1

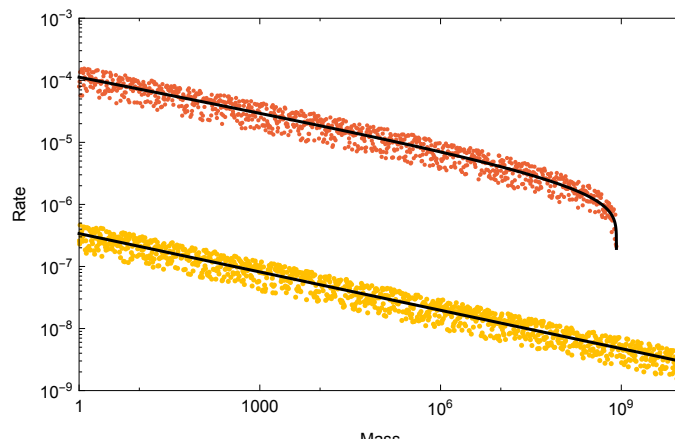


Fig. 2

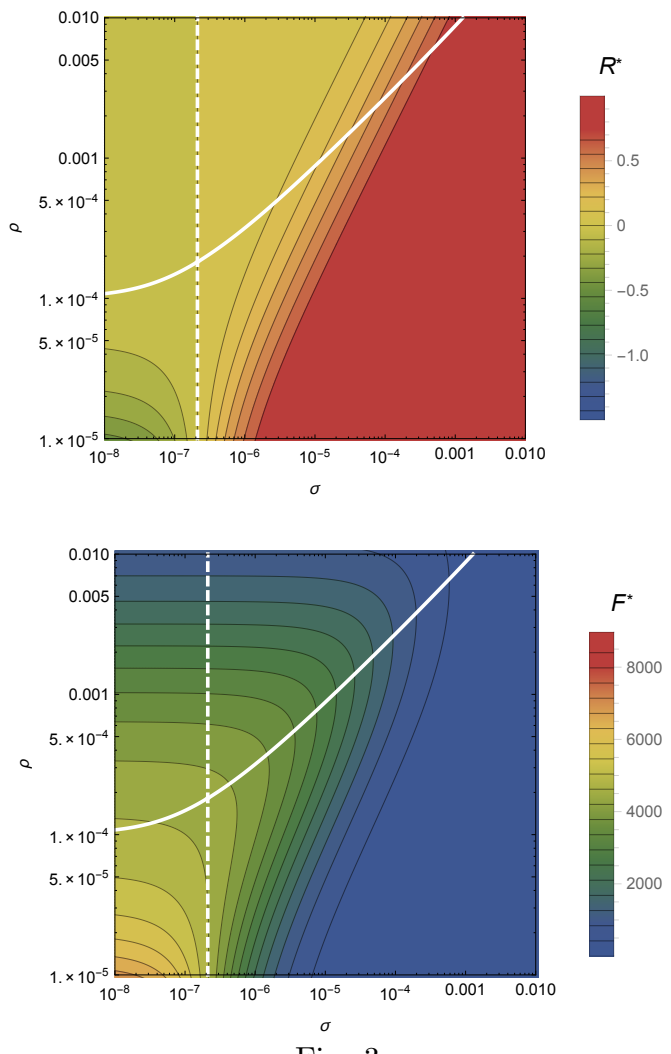


Fig. 3

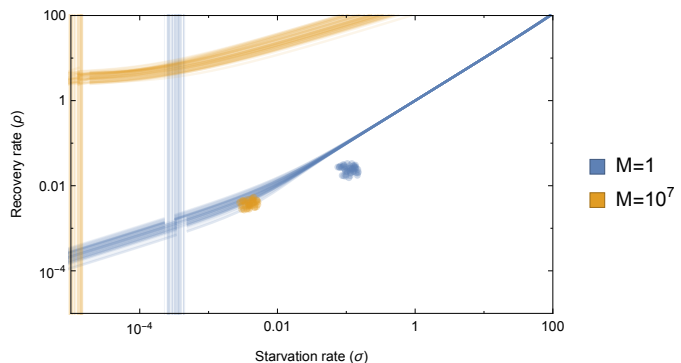


Fig. 4

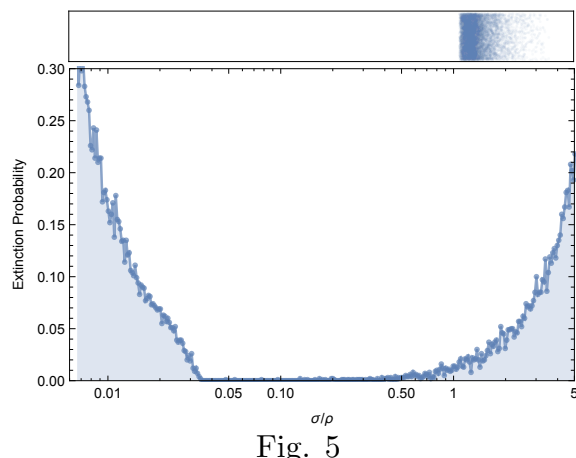


Fig. 5

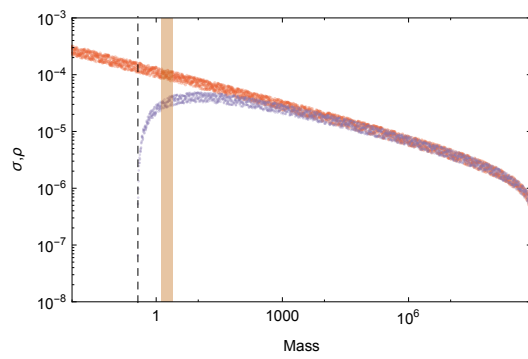
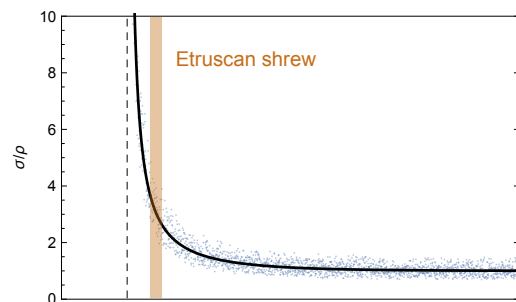
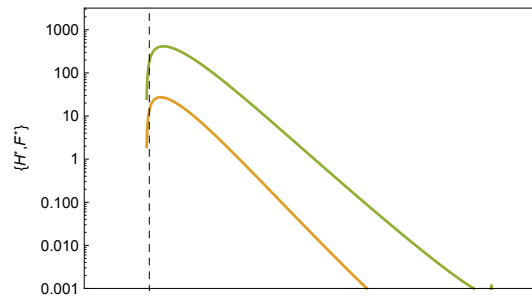


Fig. 6

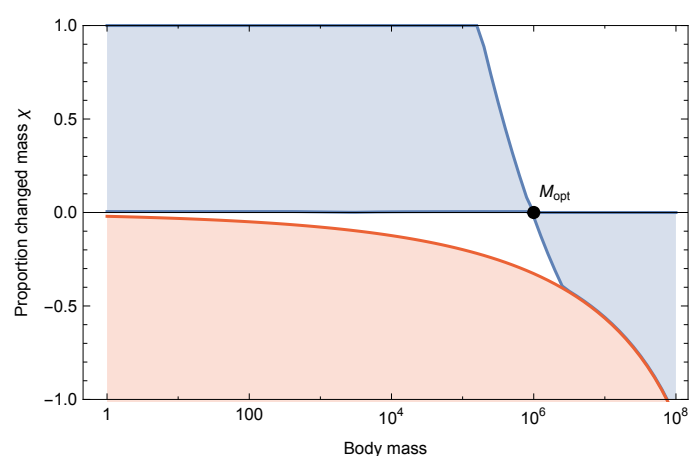


Fig. 7

Table 1: Parameter Values For Various Classes of Organisms

	Mammals	Unicellular karyotes	Eu- karyotes	Bacteria
η	3/4			1.70
E_m	10695 (J gram ⁻¹)			10695 (J gram ⁻¹)
E'_m	$\approx E_m$			$\approx E_m$
B_0	0.019 (W gram ^{-α})			1.96×10^{17}
B_m	0.025 (W gram ⁻¹)			0.025 (W gram ⁻¹)
a	1.78×10^{-6}			1.83×10^{13}
b	2.29×10^{-6}			2.29×10^{-6}
$\eta - 1$	-0.21			0.73
λ_0	3.39×10^{-7} (s ⁻¹ gram ^{1-η})			56493
γ	1.19			0.68
f_0	0.02			1.30×10^{-5}
ζ	1.01			
mm_0	0.32			